Determination of the elastic properties of SiO2 nanotubes templated from organic amphiphilic self-assemblies through inorganic transcription

Saïd Houmadi, Dimitri Dedovets, Satyabrata Si, Tamoto Rumi, Reiko Oda, Marie-Hélène Delville, Christian Bergaud

AIP | Applied Physics Letters

Determination of the elastic properties of SiO2 nanotubes templated from organic amphiphilic self-assemblies through inorganic transcription

S. Houmadi, D. Dedovets, S. Si, R. Tamoto, R. Oda et al.

Citation: Appl. Phys. Lett. **102**, 151904 (2013); doi: 10.1063/1.4801760
View online: http://dx.doi.org/10.1063/1.4801760
View Table of Contents: http://apl.aip.org/resource/1/APPLAB/v102/i15
Published by the American Institute of Physics.

Determination of the elastic properties of SiO_2 nanotubes templated from organic amphiphilic self-assemblies through inorganic transcription

S. Houmadi,[1,2] D. Dedovets,[3,4,5] S. Si,[4] R. Tamoto,[3,5] R. Oda,[3,5] M. H. Delville,[4] and C. Bergaud[1,2]

[1]*CNRS, LAAS, 7 avenue du Colonel Roche, BP 54200, F-31031 Toulouse cedex 4, France*
[2]*Univ de Toulouse, LAAS, F-31400 Toulouse, France*
[3]*Chimie et Biologie des Membranes et des Nanoobjets, Université de Bordeaux-CNRS UMR 5248, Allée St Hilaire, Bat B14, 33607 Pessac, France*
[4]*CNRS, Université de Bordeaux, ICMCB, 87 avenue du Dr. A. Schweitzer, Pessac F-33600, France*
[5]*Institut Européen de Chimie et Biologie, 2 rue Robert Escarpit, 33607 Pessac, France*

(Received 21 October 2012; accepted 29 March 2013; published online 15 April 2013)

Amorphous SiO_2 nanotubes (NTs) with outer and inner diameters of 35 ± 4 nm and 10 ± 4 nm, respectively, were synthesized through inorganic transcription using organic amphiphilic self-assemblies as templates. By performing three-point bending tests on suspended SiO_2 NTs using an atomic force microscope, their elastic modulus was determined to be 73.3 ± 6.7 GPa which is comparable to that of bulk SiO_2 as well as amorphous SiO_2 nanowires obtained using chemical vapor deposition. These measurements were validated using finite element method calculations and show the crucial role played by the clamping conditions to determine the actual Young's modulus.
 [http://dx.doi.org/10.1063/1.4801760]

The achievement of nanoscale electronics is a subject of great priority for industrial technology. One of the major problems in this regard is that modern techniques based on top-down optical lithography have become drastically sophisticated with attempts to achieve further miniaturization. Alternative routes toward nanoscale electronics include the elaboration of nano-objects employed as building blocks for electronic devices via bottom-up approaches. Among them, inorganic nanotubes (NTs) have attracted a great interest in the scientific and engineering communities due to their anisotropic physical, chemical, and mechanical properties. To date, various synthetic strategies have been developed to fabricate such one-dimensional (1D) nanostructures, including physical and chemical routes along with the use of different precursors and templates.[1] Recently, chemical synthesis of inorganic nano-objects, hardly achievable by conventional or lithographic techniques,[2] has emerged as a powerful alternative to fabricate 1D nanostructures with various morphologies including twisted ribbons, nanohelices, and NTs with a precise control in terms of size, shape, and orientation.[3] For example, the chemical approach based on the structural diversity of self-assembled amphiphilic organic molecules allows developing simple synthetic strategies and obtaining complex artificial patterns and architectures at the nanoscale.[4–6]

It is of paramount importance to determine the mechanical properties of such 1D nanostructures before using them as building blocks for designing nanoelectromechanical systems (NEMS) since they dictate the overall behavior of the nanodevice in both static and dynamic regimes. Their striking features can make them key elements for many applications including ultra-sensitive mass and force sensing,[7,8] ultra-low power radio frequency signal generation and timing, and energy harvesting,[9] as well as for fundamental studies in quantum mechanics.[8] Among the various techniques employed for determining mechanical properties of 1D nanostructures are robotic nano-manipulation in scanning electron microscopy (SEM),[10] transmission electron microscopy (TEM),[11,12] and atomic force microscopy (AFM). Among them, the AFM remains the technique of choice because of its high spatial resolution and force-sensing capabilities.[13–16] Until now, AFM-based nanoindentation techniques have been used to determine the Young's modulus of nanostructures such as ZnO nanowires[17] and nanobelts,[18] but the bending technique is a more documented approach for determining the Young's modulus of 1D nanostructures.[13,14,19–23]

Whilst several studies have been devoted to the mechanical characterization of inorganic 1D nanowires and NTs[10,12,13] obtained from inorganic templates, sol-gel chemistry, or chemical vapor deposition routes,[1] little if any is known concerning the effect of the clamping conditions on the estimation of the Young's modulus of inorganic NTs using the bending technique.

In this study, we describe the determination of the Young's modulus of amorphous SiO_2 NTs synthesized through inorganic transcription using organic amphiphilic assemblies as templates. Their mechanical properties were determined by performing bending tests using atomic force spectroscopy (AFS) along with finite element method (FEM) calculations in order to evaluate the effect of the clamping conditions on the mechanical behavior. FEM was chosen because the appropriate clamping conditions can accurately be imposed and the actual geometry of the NT can be easily modeled.

Amorphous silica nanotubes were transcribed from self-assembled amphiphilic molecules.[4] These amphiphiles are cationic bis-quaternary ammonium gemini surfactants of chemical formula C_2H_4-1,2-$((CH_3)_2N^+C_{16}H_{33})_2$ which in the presence of chiral tartrate counter-anions form a gel in water by creating an extended network of nanometric twisted or helical ribbons or tubules with tunable shapes and

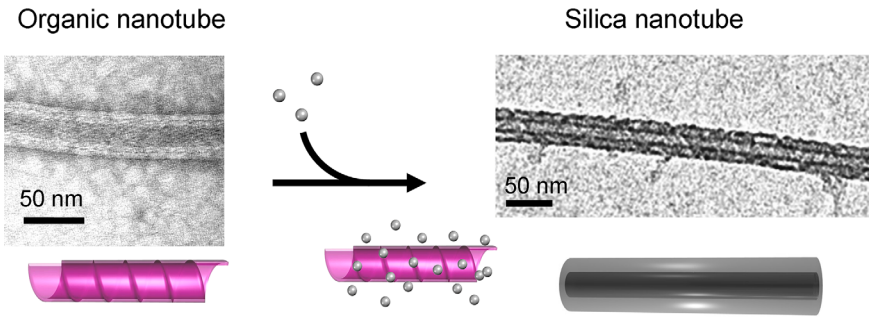

FIG. 1. TEM images of self-assembled organic NT (drawn as a pink tube) and silica NT (drawn as a grey tube) after sol-gel transcription. Grey dots in the scheme represent silica precursors which polymerize at the surface of organic silica NTs.

sizes.[24–26] We succeeded in transcribing these organic nano-assemblies into inorganic nano-objects with tunable shapes. Various parameters such as the temperature, the solvent, or the aging times were checked. An aging time of 3 days is sufficient for the organic gels to form organic nanotubes. It must be extended to 45 days so as to obtain resulting inorganic fibers with the same tubular structure. The silica precursor (tetraethylorthosilicate (TEOS)) is then added in the organic gel leading after hydrolysis and condensation to the inorganic NTs as shown in Fig. 1.

After transcription, the NTs were washed with ethanol 5 times in order to remove the non reacted precursors and organic compounds. The presence/absence of the organic compounds was controlled by FT-IR measurements. After washing for 3 times already, no signal corresponding to the CH_2 groups (organic compounds) was observed. The NTs were dispersed in ethanol, and the solution was sonicated for 10 min and then dropped onto oxidized Si wafers with microcavities (inverted pyramids) obtained after photolithography and KOH etching. The width of the cavities ranges from 0.7 to 1.5 μm with a depth from 0.5 to 1.5 μm. The samples were then dried at ambient temperature.

The suspended NTs were first imaged and located using SEM images (Hitachi S-4800 high resolution SEM). The chosen ones were clamped by the Ion Beam-Induced Deposition (IBID) technique using Pt pads to get rid of any sliding effect or lift-off when performing the bending test. Various clamping conditions were also assessed by FEM simulations for estimating the Young's modulus of the NT. AFM images were recorded in Tapping mode, and force vs. vertical displacement (F-d) curves were obtained in ScanAsyst mode using Dimension Icon AFM from Bruker, in air at room temperature. This technique, instead of contact mode, allows imaging at very low interaction forces and without lateral friction since it performs a very fast F-d curve at every pixel in the image with a direct force control.

The AFM bending test was used to determine the Young's modulus of the clamped SiO_2 NTs. This technique, developed by several groups to determine the mechanical properties of nanofilaments, tubes, and wires,[13,14,19,21,27] involves the use of doubly clamped NTs positioned over trenches or cavities and subjected to an applied load using an AFM. NTs are pushed precisely at their midpoint with calibrated Si_3N_4 cantilevers, and the *F-d* curve is recorded. Fig. 2 shows a typical example of an AFM topographic image and the corresponding SEM image of a suspended SiO_2 NT over a microcavity. Several SiO_2 NTs were investigated, and repeated *F-d* curves were performed for each NT using different AFM tips.

Figure 3(a) shows three typical *F-d* curves recorded for a SiO_2 NT with an outer diameter of 35 ± 4 nm (as obtained by AFM, Figure 4(a)) and inner diameter of 10 ± 4 nm (as obtained by TEM tomography). The similarity of the two curves obtained for the substrate itself (black curve) and for

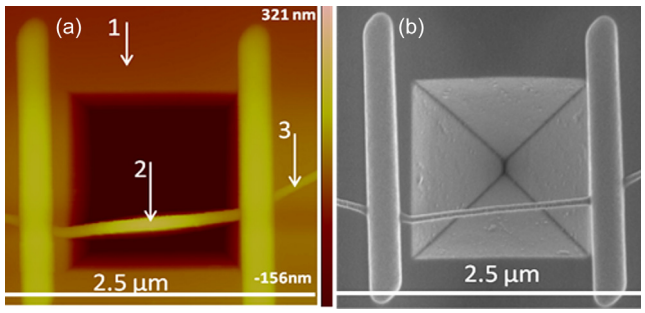

FIG. 2. (a) Tapping mode AFM image of a SiO_2 NT suspended above a microcavity of a Si substrate and clamped at its extremities. (b) SEM image of the same NT.

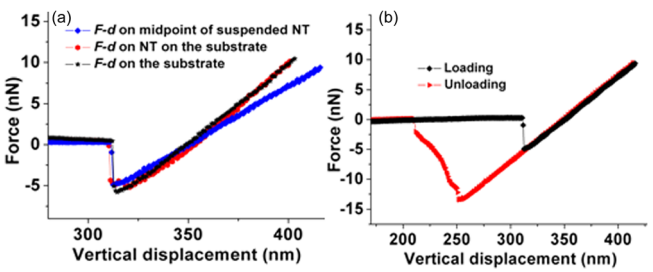

FIG. 3. (a) Typical *F-d* curves obtained on the substrate indicated by arrow 1 in Fig. 2 (black color), on a suspended NT loaded at its midpoint indicated by arrow 2 in Fig. 2 (blue color), on the same NT positioned on the substrate indicated by arrow 3 in Fig. 2 (red color). *(b)* Typical *F-d* curve of a suspended NT showing approach (in black) and retract (in red). The hysteresis is due to the adhesion force.

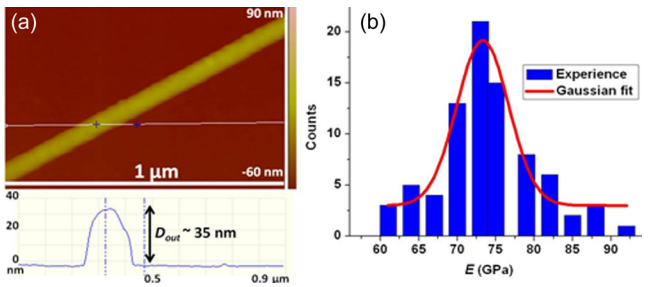

FIG. 4. (a) Tapping mode AFM image of an isolated SiO_2 NT on the Si substrate and its corresponding cross section giving an outer diameter D_{out} about 35 nm. (b) Histogram showing the distribution of the elastic modulus after repetitive F-d curve measurements.

the portion of the NT in contact with the substrate (red curve) shows that squeezing effect or indentation induced by the AFM tip on the NT can be considered as negligible. Indeed, the typical apex radius of curvature (ca. 20 nm) is supposed to limit the tip indentation onto the NTs because of its comparable radius.

The third *F-d* curve was obtained at the midpoint of the suspended NT. In the non-contact region, while the AFM tip approaches the NT, the *F-d* curve shows no deflection. As the tip is brought very close to the surface, it jumps into contact with the NT; from this point the force increases linearly as the NT is loaded. The slope of the *F-d* curve remains in the linear regime at low forces ($F \leq 10$ nN) showing that the mechanical behavior of the NT is elastic in this range of applied forces. The unloading step then occurs when the tip reverses direction (Fig. 3(b), red track). It can be seen that the loading-unloading curves are well superposed in the linear regime, except for the hysteresis due to the adhesion force at the contact.

The elastic modulus E was then determined using the beam bending theory of clamped-clamped beam.[28] The relationship between E and the elastic deformation of a cylindrical beam or tube of suspended length L (measured from AFM and SEM images in our case) subjected to a load f at its midpoint is given by

$$E = \frac{f}{\Delta z}\frac{L^3}{192I}, \tag{1}$$

where I is the moment of inertia given by $I = \frac{\pi(D_{out}^4 - D_{in}^4)}{64}$ for a tube with outer and inner diameters D_{out} and D_{in}, respectively.

The term $\frac{f}{\Delta Z}$ in Eq. (1) is the force per unit deflection. It is measured by the slope of the *F–d* curve as described in Ref. 14.

For all tested NTs prepared with clamping conditions where both ends of the SiO_2 NT are clamped at the edges of the cavity (Fig. 2(a)), the calculated values of E ranged from 61 to 92 GPa. These values are displayed in Fig. 4(b) as a histogram showing the cumulative occurrence of the Young's modulus obtained from repetitive *F-d* curves. The average value E and its standard deviation were determined by fitting the histogram with a Gaussian curve. This analysis yields an average value of 73.3 ± 6.7 GPa which is in good agreement with that of the bulk (73 GPa)[29] and with the reported value of 76.6 ± 7.2 GPa measured by three-point bending tests for amorphous SiO_2 nanowires with a diameter ranging from 50 nm to 100 nm and synthesized using chemical vapor deposition (CVD).[30]

This result is also close to the reported value of 75 GPa measured from contact-resonance AFM for Si nanowires with diameters less than 60 nm and oxidized through a rapid thermal oxidation.[31] However, the calculated E is lower than the elastic modulus of 144 GPa obtained by nanoindentation technique for plasma-enhanced CVD (PECVD) SiO_2 thin films[32] and slightly higher than both the average values of 60.1 ± 3.4 GPa obtained by digital imaging method from SiO_2 films deposited using PECVD[33] and of 59 GPa determined by the thermal stress of SiO_2 fine lines on a Si substrate.[34] This discrepancy may be due to differences in preparation procedures; it has indeed been reported that the density of CVD SiO_2 is lower than that of thermally grown one.[35] It can also be attributed to the testing methods and the boundary conditions.[36]

To address this issue, the bending of such SiO_2 NT was also estimated by FEM calculations using the COMSOL MULTIPHYSICS Software. As shown in Fig. 5, the NT was modeled as a perfect tube with the same dimensions as those used in the experiments (i.e., 1 μm-long with outer and inner diameters of 36 nm and 10 nm, respectively). The extremities of the NT are clamped in position so as to correspond to the experimental clamping, and a normal force of $F = 10$ nN is applied in the midpoint in order to assure symmetrical bending of the NT. As shown in Table I, the NT bending obtained from FEM calculations for different lengths using the E value extracted from experimental measurements is in very good agreement with the one measured from *F-d* curves.

Nonetheless, when the bending tests are performed on suspended NTs with clamping conditions similar to those shown in Fig. 6 (i.e., clamping boundaries of the NTs far from the edge of the microcavity), we noticed that the E values were higher than the reported values[29,30] and further increased as the distance between the clamped location and the edge of the microcavity increased, varying from 100 to 280 GPa.

To further investigate the effect of the boundary conditions on the measured Young's modulus, different clamping conditions were simulated and examined in detail. In Fig. 7 is shown a 1.5 μm-long NT with outer and inner diameters of

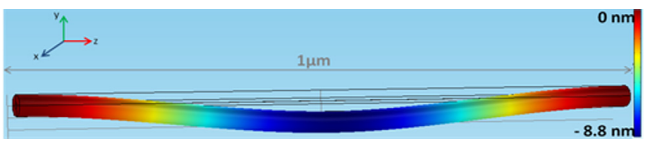

FIG. 5. FEM simulation of a clamped NT with a length of 1 μm and an outer diameter of 36 nm subjected to a load of 10 nN at the midpoint.

TABLE I. Summary of NT bendings calculated from FEM and from AFM measurements with a normal force of 10 nN applied at the midpoint of the NT.

Tube length (μm)	Bending Δz (nm) from FEM	Bending Δz (nm) from *F-d* curves
1	9	11 ± 1
1.2	15	17 ± 2
1.4	24	26 ± 2

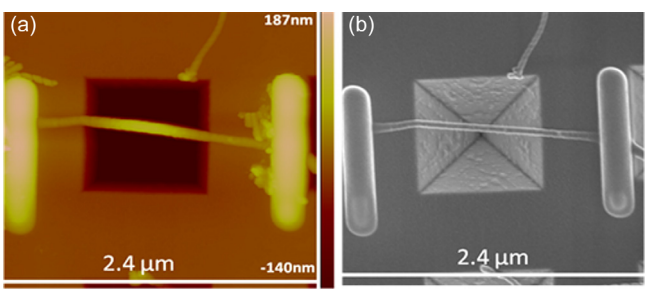

FIG. 6. (a) AFM and (b) SEM images of a suspended NT with non ideal clamping conditions.

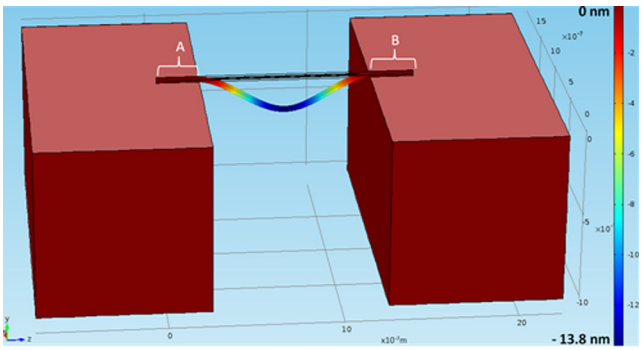

FIG. 7. The FEM simulation of a clamped NT with a length of 1.5 μm and an outer diameter of 36 nm subjected to a load of 10 nN at the midpoint. Portions of the tube (250 nm each) indicated by the curly brackets A and B are in contact with the substrate.

36 nm and 10 nm, respectively. The extremities of the NT are clamped so that only 1 μm of the NT is suspended over the cavity. As in the previous experiments, the NT was bent by applying a normal force of $F = 10$ nN in the midpoint. In Table II are given the bending calculated from FEM and the corresponding elastic moduli compared to those extracted from *F-d* curves for a NT of 1.5 μm in length with different clamping conditions. As shown in Fig. 7, the NT bending is about 14 nm. This value is much smaller than the one obtained for clamping conditions corresponding to Fig. 2 (i.e., 31 nm). This discrepancy can be explained by a partial loss of the mechanical energy likely due to stretching in the portion of the NT positioned on the substrate before the clamped ends (lengths A and B on Fig. 7). This gives rise to a smaller deflection of the suspended part of the NTs for an identical applied load and therefore leads to an overestimation of the elastic modulus *E*.

These results demonstrate the importance of the clamping conditions on the bending test measurements and their direct impact on the extraction of the elastic properties of 1D nanostructures. Under conditions where the total length of the NT is equal to its suspended part, provided the extremities of the NT are clamped, a good estimation of the elastic modulus *E* can be obtained using the beam bending theory of clamped-clamped beam. Otherwise, as shown by FEM calculations, the elastic modulus is always overestimated.

In conclusion, topographical information and diameter of individual amorphous SiO_2 NTs obtained by an inorganic transcription were determined by AFM measurements. Experimental and numerical approaches were used to accurately determine their actual elastic properties. Clamping conditions of the NTs were found to play a crucial role in the extraction of the elastic modulus. We envisage now to use other nanometric objects using templates with different morphologies such as twisted or helical ribbons in a controlled and hierarchical manner for designing functional NEMS. Protocols using techniques as different as Atomic Layer Deposition (ALD) and sol-gel chemistry will be implemented.

TABLE II. Summary of NT bendings calculated from FEM and its corresponding elastic modulus compared to those extracted from *F-d* curves obtained with a normal force of 10 nN applied at the midpoint of a NT with a length of 1.5 μm with different clamping conditions.

	Clamping boundaries of the NT far from the edge of the cavity	Clamping boundaries of the NT at the edge of the cavity
Bending Δz (nm) from FEM	14	31
Bending Δz (nm) from *F-d* curves	16 ± 2	33 ± 2
E (GPa)	165	73.3

This work was supported by the NANOSPRINGS project (Grant No. ANR-10-BLANC-0813) of the Agence Nationale pour la Recherche. S. Houmadi, D. Dedovets, and S. Si acknowledge the ANR for their grants. This work was partly supported by the French RENATECH network.

[1]C. N. R. Rao and A. Govindaraj, Adv. Mater. **21**, 4208 (2009).
[2]L. Zhang, E. Ruh, D. Grutzmacher, L. Dong, D. J. Bell, B. J. Nelson, and C. Schonenberger, Nano Lett. **6**, 1311 (2006).
[3]Y. Qiao, Y. Wang, Z. Yang, Y. Lin, and J. Huang, Chem. Mater. **23**, 1182 (2011).
[4]T. Delclos, C. Aimé, E. Pouget, A. Brizard, I. Huc, M. H. Delville, and R. Oda, Nano Lett. **8**, 1929 (2008).
[5]R. Kiagus-Armad, A. Brizard, C. Tang, R. Blatchly, B. Desbat, and R. Oda, Chem. Eur. J. **17**, 9999–10009 (2011).
[6]C. Aime, R. Tamoto, T. Satoh, A. Grelard, E. J. Dufourc, T. Buffeteau, H. Ihara, and R. Oda, Langmuir **25**, 8489–8496 (2009).
[7]B. Ilic, Y. Yang, and H. G. Craighead, Appl. Phys. Lett. **85**, 2604 (2004).
[8]R. He, X. L. Feng, M. L. Roukes, and P. Yang, Nano Lett. **8**, 1756 (2008).
[9]Y. Zhang, Y. Liu, and Z. L. Wang, Adv. Mater. **23**, 3004 (2011).
[10]D. A. Smith, V. C. Holmberg, and B. A. Korge, ACS Nano **4**, 2356 (2010).
[11]P. Poncharal, Z. L. Wang, D. Ugarte, and W. A. de Heer, Science **283**, 1513 (1999).
[12]R. Gao, Z. L. Wang, Z. Bai, W. A. de Heer, L. Dai, and M. Gao, Phys. Rev. Lett. **85**, 622 (2000).
[13]B. Wu, A. Heidelberg, and J. J. Boland, Nature Mater. **4**, 525 (2005).
[14]Q. Xiong, N. Duarte, S. Tadigadapa, and P. C. Eklund, Nano Lett. **6**, 1904 (2006).
[15]Y. J. Kim, K. Son, I. C. Choi, I. S. Choi, W. I. Park, and J. i. Jang, Adv. Funct. Mater. **21**, 279 (2011).
[16]Z. H. Xu and X. Li, Adv. Funct. Mater. **21**, 3883 (2011).
[17]G. Stan, C. V. Ciobanu, P. M. Parthangal, and R. F. Cook, Nano Lett. **7**, 3691 (2007).
[18]H. Ni and X. Li, Nanotechnology **17**, 3591 (2006).
[19]B. Wen, J. E. Sader, and J. J. Boland, Phys. Rev. Lett. **101**, 175502 (2008).
[20]J. F. Smith, T. P. J. Knowles, C. M. Dobson, C. E. MacPhee, and M. E. Welland, Proc. Natl. Acad. Sci. U.S.A. **103**, 15806 (2006).
[21]Y. Qin, Y. Kim, L. Zhang, S. M. Lee, R. B. Yang, A. Pan, K. Mathwig, M. Alexe, U. Gösele, and M. Knez, Small **6**, 910 (2010).
[22]S. Cuenot, S. Demoustier-Champagne, and B. Nysten, Phys. Rev. Lett. **85**, 1690 (2000).
[23]A. Heidelberg, L. T. Ngo, B. Wu, M. A. Phillips, S. Sharma, T. I. Kamins, J. E. Sader, and J. J. Boland, Nano Lett. **6**, 1101 (2006).
[24]R. Oda, F. Artzner, M. Laguerre, and I. Huc, J. Am. Chem. Soc. **130**, 14705 (2008).
[25]R. Oda, I. Huc, M. Schmutz, S. J. Candau, and F. C. MacKintosh, Nature (London) **399**, 566 (1999).
[26]A. Brizard, C. Aime, T. Labrot, I. Huc, D. Berthier, F. Artzner, B. Desbat, and R. Oda, J. Am. Chem. Soc. **129**, 3754 (2007).
[27]M. Zheng, X. Chen, I. T. Bae, C. Ke, C. Park, M. W. Smith, and K. Jordan, Small **8**, 116 (2012).
[28]J. M. Gere and S. P. Timoshenko, *Mechanics of Materials*, 3rd ed. (PWS-KENT, Boston, Massachusetts, 1990).
[29]B. Bhushan, *Handbook of Nanotechnology*, 2nd ed. (Springer, Berlin, 2007), p. 1040.
[30]H. Ni, X. Li, and H. Gao, Appl. Phys. Lett. **88**, 043108 (2006).
[31]G. Stan, S. Krylyuk, A. V. Davydov, and R. F. Cook, Nano Lett. **10**, 2031 (2010).
[32]X. Li, B. Bhushan, K. Takashima, C. W. Baek, and Y. K. Kim, Ultramicroscopy **97**, 481 (2003).

[33]W. N. Sharpe, J. Pulskamp, D. S. Gianola, C. Eberl, R. G. Polcawich, and R. J. Thompson, Exp. Mech. **47**, 649 (2007).
[34]J. H. Zhao, T. Ryan, P. S. Ho, A. J. McKerrow, and W. Y. Shih, J. Appl. Phys. **85**, 6421 (1999).
[35]N. Awaji, S. Ohkubo, T. Nakanishi, T. Aoyama, Y. Sugita, K. Takasaki, and S. Komiya, Appl. Phys. Lett. **71**, 1954 (1997).
[36]Q. Q. Qin, F. Xu, Y. Cao, P. I. Ro, and Y. Zhu, Small **8**, 2571 (2012).